

## Non-Fermi liquid behavior in the filled skutterudite compound $\text{CeRu}_4\text{As}_{12}$

This article has been downloaded from IOPscience. Please scroll down to see the full text article.

2008 J. Phys.: Condens. Matter 20 075110

(<http://iopscience.iop.org/0953-8984/20/7/075110>)

View [the table of contents for this issue](#), or go to the [journal homepage](#) for more

Download details:

IP Address: 129.252.86.83

The article was downloaded on 29/05/2010 at 10:33

Please note that [terms and conditions apply](#).

# Non-Fermi liquid behavior in the filled skutterudite compound CeRu<sub>4</sub>As<sub>12</sub>

R E Baumbach<sup>1</sup>, P C Ho<sup>1</sup>, T A Sayles<sup>1</sup>, M B Maple<sup>1</sup>, R Wawryk<sup>2</sup>,  
T Cichorek<sup>2</sup>, A Pietraszko<sup>2</sup> and Z Henkie<sup>2</sup>

<sup>1</sup> Department of Physics and Institute for Pure and Applied Physical Sciences, University of California at San Diego, La Jolla, CA 92093, USA

<sup>2</sup> Institute of Low Temperature and Structure Research, Polish Academy of Sciences, 50-950 Wrocław, Poland

Received 10 August 2007, in final form 7 December 2007

Published 31 January 2008

Online at [stacks.iop.org/JPhysCM/20/075110](http://stacks.iop.org/JPhysCM/20/075110)

## Abstract

Electrical resistivity  $\rho$ , specific heat  $C$ , and magnetic  $M$  measurements made on the filled skutterudite CeRu<sub>4</sub>As<sub>12</sub> reveal non-Fermi liquid (NFL) temperature dependences at low  $T$ , i.e.  $\rho(T) \sim T^{1.4}$  and weak power law or logarithmic divergences in  $C(T)/T$  and  $M/H = \chi(T)$ . Measurements also show that the temperature dependence of the thermoelectric power  $S(T)$  deviates from that seen in other Ce systems. The NFL behavior appears to be associated with a nonmagnetic ground state, as revealed by magnetization  $M(H, T)$  measurements.

## 1. Introduction

The filled skutterudite compounds of the form MT<sub>4</sub>X<sub>12</sub> (M = alkali metal, alkaline earth, lanthanide, actinide; T = Fe, Ru, Os; X = P, As, Sb) exhibit a wealth of strongly correlated electron phenomena including spin fluctuations, itinerant ferromagnetism, local moment ferromagnetism and antiferromagnetism, conventional BCS (Bardeen–Cooper–Schrieffer) superconductivity, unconventional superconductivity, heavy-fermion behavior, and non-Fermi liquid behavior [1, 2]. Many of these phenomena depend on hybridization between the rare earth or actinide f-electron states and the conduction electron states. This trend is evident in the CeT<sub>4</sub>X<sub>12</sub> systems, most of which are semiconductors where the gap size is correlated with the lattice constant [3–5]. The effects of hybridization are particularly dramatic for CeRu<sub>4</sub>Sb<sub>12</sub> which, until now, was the only filled skutterudite known to show non-Fermi liquid (NFL) behavior [6–8]. In this compound, the NFL behavior is characterized at low  $T$  as follows: resistivity— $\rho(T) \sim T^{1.4}$ , specific heat divided by temperature— $C(T)/T \sim -\ln T$  or  $T^{-0.58}$ , and magnetic susceptibility— $\chi(T) \sim T^{-0.35}$ , all of which suggest that CeRu<sub>4</sub>Sb<sub>12</sub> is located near a quantum critical point (QCP). The value of the lattice constant for CeRu<sub>4</sub>Sb<sub>12</sub> at room temperature indicates that the Ce ions are nearly trivalent, suggesting that a Kondo lattice description is appropriate for this compound.

In this paper, we present measurements of  $\rho(T)$ ,  $C(T)$ , magnetization  $M(H, T)$ , and thermoelectric power  $S(T)$  for CeRu<sub>4</sub>As<sub>12</sub> which show unusual behavior at and below room

temperature. The  $M(H, T)$  measurements indicate that the Ce ions have a nonmagnetic ground state. We also discuss evidence for NFL behavior at low  $T$  and suggest that this compound may be near to a QCP that has been suppressed to 0 K.

## 2. Experimental details

Single crystals of CeRu<sub>4</sub>As<sub>12</sub> were grown from elements with purities of  $\geq 99.9\%$  by a molten metal flux method at high temperatures and pressures, the details of which will be reported elsewhere [9]. After removing the majority of the flux by distillation, CeRu<sub>4</sub>As<sub>12</sub> single crystals of an isometric form with dimensions of up to  $\sim 0.7$  mm were collected and cleaned in acid in an effort to remove any impurity phases from the surfaces of the crystals. The crystal structure of CeRu<sub>4</sub>As<sub>12</sub> was determined by x-ray diffraction on a crystal with dimensions of  $0.17 \times 0.18 \times 0.23$  mm. A total of 5714 reflections (447 unique,  $R_{\text{int}} = 0.0772$ ) were recorded and the structure was resolved by the full matrix least squares method using the SHELX-97 program with a final discrepancy factor  $R_1 = 0.0273$  [for  $I > 2\sigma(I)$ ,  $wR_2 = 0.0619$ ] [10, 11].

Electrical resistivity  $\rho(T)$  measurements for  $65 \text{ mK} < T < 290 \text{ K}$  were performed in a four-wire configuration in zero magnetic field using a conventional <sup>4</sup>He cryostat and a <sup>3</sup>He–<sup>4</sup>He dilution refrigerator. Magnetization  $M(H, T)$  measurements for  $1.9 \text{ K} < T < 300 \text{ K}$  and  $0 < H < 55 \text{ kOe}$  were conducted using a Quantum Design magnetic properties measurement system on mosaic of crystals ( $m = 121 \text{ mg}$ )

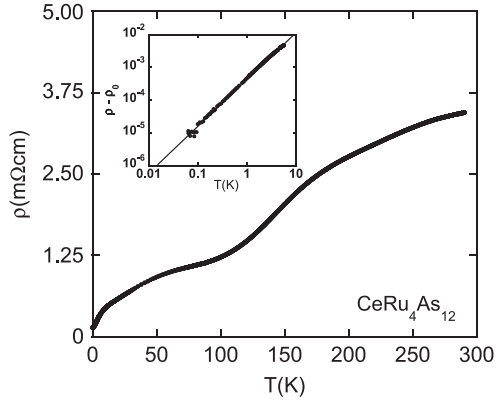


**Figure 1.** Electrical resistivity  $\rho$  versus temperature  $T$  for  $\text{CeRu}_4\text{As}_{12}$ . Inset: log-log plot of  $\rho - \rho_0$  versus  $T$  between 65 mK and 10 K, where  $\rho_0$  is the residual resistivity. The data can be described by the expression  $\rho(T) = \rho_0 + AT^n$ , where  $\rho_0 = 136 \mu\Omega \text{ cm}$ ,  $A = 19.0 \mu\Omega \text{ cm K}^{-n}$  and  $n = 1.4$  (straight line in the figure).

**Table 1.** Atomic coordinates, displacement parameters, and occupancy factors for  $\text{CeRu}_4\text{As}_{12}$ .  $U_{\text{eq}}$  is defined as one-third of the trace of the orthogonalized  $U_{ij}$  tensor.

Atom	$x$	$y$	$z$	$U_{\text{eq}}$ ( $\text{\AA}^2 \times 10^{-3}$ )	Occupancy factor
Ru	0.25	0.25	0.25	3(1)	1.00(2)
As	0.1495(1)	0.3499(1)	0	4(1)	0.99(2)
Ce	0	0	0	11(1)	0.99(2)

which were mounted on a small Delrin disc using Duco cement. Specific heat  $C(T)$  measurements for  $650 \text{ mK} < T < 10 \text{ K}$  were made using a standard heat pulse technique on a collection of 11 single crystals ( $m = 45 \text{ mg}$ ) attached to a sapphire platform with a small amount of Apiezon N grease in a  $^3\text{He}$  semi-adiabatic calorimeter. The thermoelectric power  $S(T)$  for  $0.5 \text{ K} < T < 350 \text{ K}$  of  $\text{CeRu}_4\text{As}_{12}$  single crystals with a length of less than 1 mm was determined by the method described in [12].

### 3. Results

Single-crystal structural refinement shows that the unit cell of  $\text{CeRu}_4\text{As}_{12}$  has the  $\text{LaFe}_4\text{P}_{12}$ -type structure ( $Im\bar{3}$ ) space group with two formula units per unit cell, and a lattice constant  $a = 8.5004(4) \text{ \AA}$ , in reasonable agreement with earlier measurements of  $a = 8.4908 \text{ \AA}$  and  $a = 8.4963 \text{ \AA}$  [4, 5, 13]. Other crystal structure parameters are summarized in table 1. The displacement parameter  $U_{\text{eq}}$  represents the average displacement of an atom vibrating around its lattice position and is equal to its mean-square displacement along the Cartesian axes. The displacement parameters determined for  $\text{CeRu}_4\text{As}_{12}$  exhibit behavior that is typical of the lanthanide-filled skutterudites [14, 15]. Table 1 also indicates that the Ce and As sites in  $\text{CeRu}_4\text{As}_{12}$  may not be fully occupied, since there is  $\sim 2\%$  uncertainty in the occupancy factors. The possible incomplete Ce or As occupancy is even more pronounced for some other crystals,

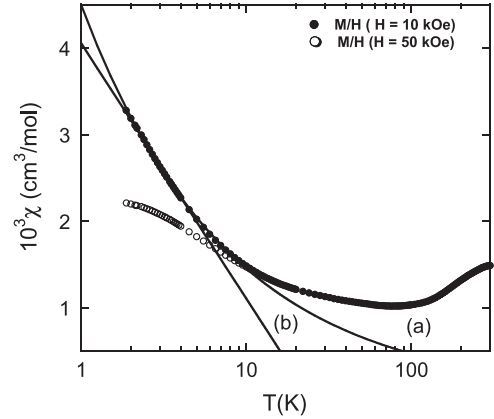


**Figure 2.** Magnetic susceptibility  $\chi$  versus temperature  $T$  for  $\text{CeRu}_4\text{As}_{12}$  between 2 and 300 K. The magnetic susceptibility  $\chi$  is defined as  $\chi = M/H$ , where  $M$  is the magnetization and  $H$  is the magnetic field, and was measured in fields of 10 kOe (filled circles) and 50 kOe (unfilled circles). For  $2 \text{ K} < T < 10 \text{ K}$ ,  $\chi(T)$  measured in a 10 kOe field is described by either a power law (curve (a)) or a logarithmic (curve (b)) function (see text).

not shown in table 1, where the Ce and As filling deviates by as much as 3% from 100% occupation.

The  $T$ -dependence of the electrical resistivity is quite unusual (figure 1). The large value of  $\rho \sim 3.5 \text{ m}\Omega \text{ cm}$  at room temperature suggests that  $\text{CeRu}_4\text{As}_{12}$  is a semi-metal. Below 300 K,  $\rho(T)$  decreases monotonically with decreasing  $T$  with negative curvature between 300 K and  $\sim 150 \text{ K}$ , positive curvature from  $\sim 150$  to  $\sim 70 \text{ K}$ , negative curvature between  $\sim 70$  and  $\sim 50 \text{ K}$ , and a semi-linear region from  $\sim 50$  to  $\sim 10 \text{ K}$ . At the lowest temperatures ( $65 \text{ mK} < T < 3.5 \text{ K}$ ),  $\rho(T)$  can be described by a power law of the form,

$$\rho(T) = \rho_0 + AT^n \quad (1)$$

where  $n = 1.4$ ,  $A = 19.0 \mu\Omega \text{ cm K}^{-n}$ , and  $\rho_0 = 136 \mu\Omega \text{ cm}$  for nearly two decades in temperature and is consistent with that seen for other NFL systems [7, 16–18]. Measurements performed on numerous samples also reveal that the qualitative behavior for  $\rho(T)$  is consistent for all samples, although variation by as much as a factor of two in the absolute value of  $\rho$  is observed, possibly due to uncertainty in the geometric factor. It should also be noted that no superconducting transition was detected above 65 mK.

Shown in figure 2 are  $\chi(T) = M(T)/H$  data measured in constant fields  $H = 10$  and 50 kOe. The  $\chi(T)$  data likewise show an unusual  $T$ -dependence in which  $\chi$  decreases rapidly with  $T$  down to  $\sim 100 \text{ K}$ , remains roughly constant down to  $\sim 65 \text{ K}$ , and then begins a slow increase down to 1.9 K which depends on the magnitude of the applied field. No part of these curves can be described by a simple Curie–Weiss law, as would be expected for magnetic  $\text{Ce}^{3+}$  ions, nor is any obvious magnetic ordering seen. For fields which fall in the linear portion of low- $T$   $M(H)$  isotherms ( $H \leq 15 \text{ kOe}$ ),  $\chi(T)$  increases continuously down to 1.9 K. In contrast, for fields above the linear portion of the low- $T$   $M(H)$  isotherm,  $\chi(T)$  tends to saturate with decreasing  $T$ , approaching a constant value near 1.9 K. The low- $T$  upturn in  $\chi(T)$  is described by

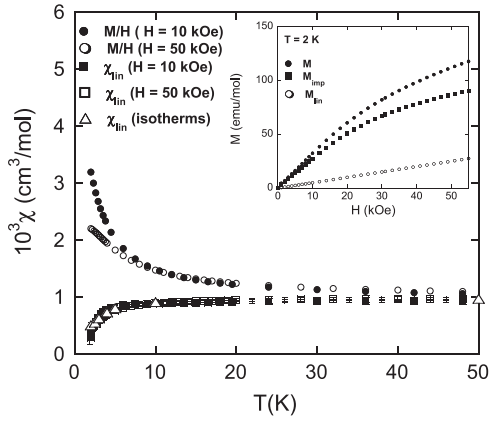


**Figure 3.** Total magnetic susceptibility  $\chi$  and intrinsic susceptibility  $\chi_{\text{lin}}$  (see text) versus temperature  $T$  for  $\text{CeRu}_4\text{As}_{12}$  between 2 K and 300 K. Inset: magnetization  $M$  versus applied field  $H$  at  $T = 2$  K. The total magnetization  $M$  is treated as a sum of a linear intrinsic magnetization  $M_{\text{lin}}$  and an impurity Brillouin function  $M_{\text{imp}}$ .

various functions, implicit in which is the assumption that the upturn is either intrinsic and due to magnetic fluctuations in the vicinity of a magnetic quantum critical point where a second-order magnetic transition has been suppressed to 0 K, or due to paramagnetic impurities embedded in a nonmagnetic host.

To consider the first viewpoint that the low-field behavior of  $\chi(T)$  is intrinsic, the  $\chi(T, H = 10 \text{ kOe})$  data were fitted below  $\sim 10$  K in a manner consistent with the NFL behavior observed in  $\rho(T)$ . Fits show that  $\chi(T)$  is described by either a power law ( $1.9 \text{ K} \leq T \leq 10 \text{ K}$ ) or a logarithmic function ( $1.9 \text{ K} \leq T \leq 6 \text{ K}$ ) of the forms,

$$\chi(T) = aT^{-m} \quad (2)$$

$$\chi(T) = b - c \ln(T) \quad (3)$$

where  $a = 4.5 \times 10^{-3} \text{ cm}^3 \text{ K}^m \text{ mol}^{-1}$  and  $m = 0.49$ , or  $b = 4.1 \times 10^{-3} \text{ cm}^3 \text{ mol}^{-1}$  and  $c = 1.3 \times 10^{-3} \text{ cm}^3 \text{ mol}^{-1}$ , respectively. This analysis assumes that the application of higher fields ( $H = 50 \text{ kOe}$ ) suppresses the low- $T$  divergence in  $\chi(T)$ , consistent with a field-induced crossover to a Fermi liquid state.

To address the possibility that the low- $T$  upturn in  $\chi(T)$  is due to magnetic impurities, isothermal  $M$  versus  $H$  measurements were made at low temperatures. As shown in the inset of figure 3, the  $M$  versus  $H$  curve for  $T = 2$  K is linear up to  $\sim 15$  kOe, develops negative curvature, and then becomes linear in higher fields. This field dependence is consistent with the total magnetization  $M$  being a sum of an intrinsic linear contribution  $M_{\text{lin}}$  that is linear in  $H$  and an impurity contribution  $M_{\text{imp}}$  that saturates at high  $H$ . For  $M(H)$  isotherms at  $T = 2, 2.5, 3, 4, 5, 10, 50, 100$  K, and  $\chi(T)$  curves at  $H = 10$  and  $50$  kOe, the impurity contribution was optimized and removed from the total magnetization in the manner described in [19]. The resulting curves are shown in figure 3, where the intrinsic susceptibilities  $M_{\text{lin}}(T)/H = \chi_{\text{lin}}(T)$  for  $H = 10$  and  $50$  kOe, as well as those taken from linear fits to the  $M_{\text{lin}}(H)$  isotherms, are shown to agree and are compared with the total susceptibilities for  $H = 10$

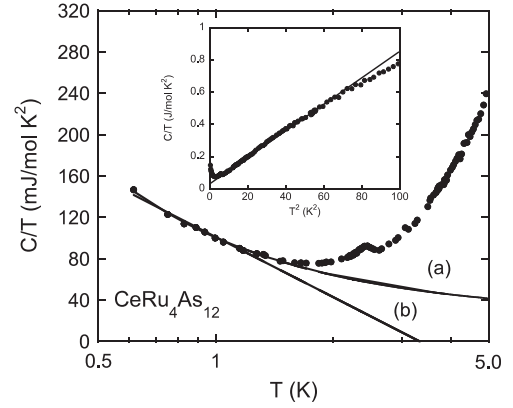


**Figure 4.** Specific heat  $C$  divided by temperature  $T$  versus  $T$  for  $\text{CeRu}_4\text{As}_{12}$ . For  $T < 2.6$  K, an upturn is observed which persists to 650 mK. The divergence conforms to a weak power law (curve (a)) or logarithmic function (curve (b)) (see text). It should be noted that a small feature is observed with a maximum at 2.4 K which appears to be related to an impurity phase. Shown in the inset is a plot of  $C/T$  versus  $T^2$  between 0.5 and 10 K. The straight line is a fit of equation (6) which yields  $\gamma = 26 \text{ mJ mol}^{-1} \text{ K}^{-2}$  and  $\theta_D = 156$  K.

and 50 kOe. In the high-temperature region,  $\chi$  and  $\chi_{\text{lin}}$  are nearly identical, since the supposed impurity contribution is small. Near 100 K, the deviation between the two quantities is noticeable as  $\chi_{\text{lin}}$  becomes constant, while  $\chi$  saturates and then begins a slow increase. Below  $\sim 10$  K,  $\chi_{\text{lin}}$  begins a gradual decrease which becomes much stronger below  $\sim 5$  K, in the range where NFL behavior in  $\rho(T)$  and  $C(T)/T$  occurs. Additionally, the fits to  $M_{\text{imp}}$  give an estimate for the impurity concentration. However, since there is no quantitative method for determining the type of magnetic impurity or whether it is of a single species or a mixture, it is necessary to assume a value for the total angular momentum  $J$ . Fits to the data assuming  $J = 8$  (Ho) and  $J = 2.5$  (Ce) yield impurity concentrations near 1% with a Landé  $g$  factor of  $g = 0.26$  and  $0.71$ , respectively. This concentration is consistent with the amount estimated from x-ray diffraction (XRD) measurements.

Displayed in figure 4 are data for specific heat divided by temperature  $C/T$  versus  $T^2$ . For  $T < 10$  K, the data decrease with temperature down to 2.6 K, below which they exhibit an upturn that persists to 650 mK. The strength of the upturn is comparable to that seen for the related NFL compound  $\text{CeRu}_4\text{Sb}_{12}$  [7]. It should be noted that a small feature with a maximum at 2.4 K is also observed. The feature is associated with an impurity component and is not seen in  $C/T$  measurements of all  $\text{CeRu}_4\text{As}_{12}$  specimens, although the other features, such as the low-temperature divergence, are seen. For temperatures  $2.6 \text{ K} < T < 8 \text{ K}$ , the data can be described by,

$$C/T = \gamma + \beta T^2 \quad (4)$$

where  $\gamma$  is the electronic specific heat coefficient and  $\beta \propto \theta_D^{-3}$  describes the lattice contribution. Fits to equation (4) to  $C(T)/T$  show that  $\gamma \sim 26 \text{ mJ mol}^{-1} \text{ K}^{-2}$  and  $\theta_D \sim 156$  K. For  $650 \text{ mK} < T < 2.6$  K,  $C/T$  diverges from the  $T^2 T$ -dependence and increases with decreasing temperature. This low-temperature divergence in  $C/T$  can

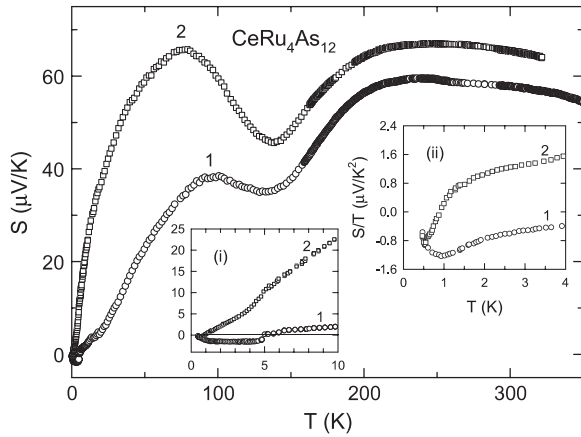


**Figure 5.** Thermoelectric power  $S$  versus temperature  $T$  for two different crystals of  $\text{CeRu}_4\text{As}_{12}$  from the same batch. Inset (i) shows  $S$  versus  $T$  between 0.47 and 10 K, while inset (ii) displays  $S/T$  versus  $T$  between 0.47 and 4 K.

be described by either a weak power law or a logarithmic function (equations (5) and (6)) where  $\gamma = 26 \text{ mJ mol}^{-1} \text{ K}^{-2}$ ,  $\phi = 74.5 \text{ mJ mol}^{-1} \text{ K}^{-(2-l)}$  and  $l = 0.97$  or  $\phi = 101 \text{ mJ mol}^{-1} \text{ K}^{-2}$  and  $\zeta = 84 \text{ mJ mol}^{-1} \text{ K}^{-2}$ , respectively. Again, the behavior is consistent with typical NFL phenomena:

$$C/T = \gamma + \phi T^{-l} \quad (5)$$

$$C/T = \phi - \zeta \ln T. \quad (6)$$

Figure 5 shows the  $T$ -dependence of the thermoelectric power  $S(T)$  for two samples of  $\text{CeRu}_4\text{As}_{12}$ , for which there is a pronounced sample dependence. In the high-temperature region, there is a two-peak structure with a broad peak around  $T_{\text{max}} = 250 \text{ K}$  which reaches  $S_{\text{max}} = 67 \text{ V K}^{-1}$  for sample 2. The broad peak is followed by a local minimum near  $\sim 150 \text{ K}$  and a sharp peak with a maximum value near  $S_{\text{max}} = 66 \text{ } \mu\text{V K}^{-1}$  at  $T_{\text{max}} \sim 75 \text{ K}$  for sample 2 and  $S_{\text{max}} = 38 \text{ } \mu\text{V K}^{-1}$  at  $T_{\text{max}} \sim 100 \text{ K}$  for sample 1. The inset figure 5(i) displays the  $T$ -dependence of  $S(T)$  below 10 K. The sample with the lower thermoelectric power exhibits an abrupt step in  $S(T)$  by about  $\Delta S_{\text{K}} \sim 2 \text{ V K}^{-1}$  near  $T^* = 5.0 \text{ K}$ . The step results in a change of sign from positive above  $T^*$  to negative below. For the sample with higher  $S(T)$ , the jump at  $T^*$  is from one nearly linear  $S(T)$  to another with a slightly lower slope. Additionally, a sign change at 0.9 K is observed for this sample. The  $S(T)$  curves for these two samples converge at an upturn near  $T = 0.47 \text{ K}$ , as shown in figure 5(ii), where the average value of  $S/T$  is equal to  $-0.6 \text{ V K}^{-2}$ .

#### 4. Discussion

Taken together, measurements of  $\rho(T)$ ,  $M(H, T)$ ,  $C(T)/T$ , and  $S(T)$  reveal anomalous types of behavior in both the high- and low-temperature regions. The decreasing magnetic susceptibility with  $T$  is particularly interesting, as it signals a transition to a nonmagnetic state at low  $T$ . There are two well-known models which describe such an evolution in magnetism. The first is the intermediate valence picture where

the Ce ions have a dynamic temporally fluctuating valence, in this case between 3+ (magnetic) and 4+ (nonmagnetic), which evolves into a nonmagnetic ground state below a characteristic ‘valence fluctuation’ temperature  $T_{\text{vf}}$ . The second is a Kondo lattice picture where the magnetic moments of  $\text{Ce}^{3+}$  ions which occupy a sublattice are screened by conduction electrons, resulting in a nonmagnetic ground state, below a characteristic ‘Kondo’ temperature  $T_{\text{K}}$ .

In the intermediate valence picture, the ratios  $n^{3+}(T)$  and  $n^{4+}(T) = 1 - n^{3+}(T)$  describe the fraction of Ce ions in each valence state. The 4f-electron shell of each Ce ion temporally fluctuates between the configurations  $4f^1$  ( $\text{Ce}^{3+}$ ) and  $4f^0$  ( $\text{Ce}^{4+}$ ) at a frequency  $\omega \approx k_{\text{B}}T_{\text{vf}}/\hbar$ , where  $T_{\text{vf}}$  separates magnetic behavior at high temperatures  $T \gg T_{\text{vf}}$  and nonmagnetic behavior at low temperatures  $T \ll T_{\text{vf}}$  [20, 21]. For  $\text{Ce}^{3+}$ , there is one localized 4f-electron and  $\chi(T)$  should behave as a Curie–Weiss law modified by the crystalline electric field (CEF) splitting of the ground state doublet and an excited state quartet by a splitting temperature  $T_{\text{CEF}}$  on the order of several hundred kelvin, as seen for other Ce-filled skutterudite compounds such as  $\text{Ce}_{0.9}\text{Fe}_3\text{CoSb}_{12}$  ( $T_{\text{CEF}} \sim 350 \text{ K}$ ) [14]. For  $\text{Ce}^{4+}$ , there is no localized f-electron and  $\chi(T)$  should behave as a Pauli susceptibility. However, for an intermediate valence state involving a temporal admixture of the  $4f^1$  and  $4f^0$  configurations,  $\chi(T)$  is expected to be intermediate between  $\chi(T)$  of the  $\text{Ce}^{3+}$  and  $\text{Ce}^{4+}$  integral valence states for  $T \gg T_{\text{vf}}$  and to exhibit an enhanced Pauli-like susceptibility for  $T \ll T_{\text{vf}}$ . Magnetic ordering can also occur if the characteristic temperature for the RKKY (Ruderman–Kittel–Kasuya–Yosida) interaction is comparable to the valence fluctuation temperature  $T_{\text{vf}}$ .

Thus, down to 90 K,  $\chi(T)$  and  $\chi_{\text{lin}}(T)$  are consistent with an intermediate valence scenario, and one in which the intermediate valence shifts in the direction of 4+ with decreasing  $T$ , as indicated by the decrease in  $\chi(T)$  with decreasing  $T$ . Comparison to other known intermediate valence compounds such as  $\text{SmS}$ ,  $\text{SmB}_6$ , or  $\text{La}_{1-x}\text{Th}_x$  doped with Ce impurities, where the Ce valence evolves from 3+ to an intermediate value as a function of Th concentration, supports this perspective [20–23]. Moreover, the intermediate valence picture is consistent with the depressed room-temperature lattice constant, as compared to the expected trivalent lanthanide contraction (LC) value for the  $\text{MRu}_4\text{As}_{12}$  series where  $M = \text{La–Pr}$  [4, 5]. To emphasize this point, a comparison can be made to the related compounds  $\text{MT}_4\text{Sb}_{12}$  and  $\text{MT}_4\text{P}_{12}$ , where  $M = \text{La–Nd}$  and  $T = \text{Fe, Ru, and Os}$ . For  $\text{MT}_4\text{Sb}_{12}$ , there is no deviation from the expected LC value at room temperature and, therefore, the Ce ions appear to have a valence near 3+, although this does not preclude the possibility of an intermediate valence state below room temperature. To probe this viewpoint, XANES (near-edge x-ray absorption fine structure) measurements have recently been made to measure the Ce valence in  $\text{CeRu}_4\text{As}_{12}$  directly. Contrary to the above discussion, the Ce ions in  $\text{CeRu}_4\text{As}_{12}$  appeared to be in the 3+ state, indicating an alternative description. These results will be discussed in detail in an upcoming publication [24].

On the other hand, the Kondo lattice picture could be appropriate if the Ce ions are trivalent and carry localized

magnetic moments. In this case, the decrease in the magnetic susceptibility with decreasing temperature indicates that the Kondo temperature  $T_K$  is above room temperature. Thus, the decrease in the resistivity with decreasing temperature could be due to a decrease in the magnetic exchange scattering consistent with the formation of the coherent Kondo lattice ground state. This scenario is expected to lead to a nonmagnetic Fermi liquid ground state. Thus, the formation of an NFL ground state would be surprising and not in agreement with the typical picture, where NFL behavior is seen in the vicinity of a magnetically ordered ground state. However, there are some f-electron systems such as  $Y_{1-x}U_xPd_3$  and  $U_{1-x}Th_xPd_2Al_3$  in which the physical properties exhibit NFL behavior at temperatures much lower than the  $T_K$  and far away from any magnetic quantum critical points [17, 18, 25, 26]. It should also be noted that if a Kondo picture is adopted, the reduced lattice constant could be explained by a Kondo-like volume collapse [27].

The high-temperature behavior is further complicated by the two-peak structure in the  $S(T)$  data. Similar two-peak structures have been observed for various other cerium systems, including the heavy-fermion system  $Ce_xY_{1-x}Cu_{2.05}Si_2$  [28], where  $x = 0.3, 0.5$ . In that case, the low- $T$  peak is ascribed to electron scattering by the ground state doublet of the  $Ce^{3+}$  ion, while the high-temperature peak is due to electronic scattering from the entire sextet of CEF levels of the  $Ce^{3+}$  ion. A more general description of  $S(T)$  for the Ce-based intermetallic systems is given by a theoretical model that takes into account the CEF splitting of the  $Ce^{3+}$  4f Hund's rule ground state multiplet and strong Coulomb repulsion of the 4f-electrons [29].

Measurements of  $\rho(T)$ ,  $M(H, T)$ , and  $C(T)/T$  also reveal an anomalous NFL state for  $CeRu_4As_{12}$  at low  $T$ . The NFL behavior is characterized by sub-quadratic power-law behavior in  $\rho(T)$ , weak power-law or logarithmic divergences in  $C(T)/T$ , and either weak power-law or logarithmic divergences in  $\chi(T)$  or a strong depression in  $\chi_{lin}(T)$  near 5 K. To quantify the NFL state roughly, a temperature scale  $T_0$  may be derived from the low-temperature fits to  $\rho(T)$ ,  $\chi(T)$  and  $C(T)/T$  using the scaled equations [17, 18, 20],

$$\rho(T) = \rho_0[1 + (T/T_{0\rho})^n] \quad (7)$$

$$\chi(T) = -B \ln(T/T_{0\chi}) \quad (8)$$

$$C(T)/T = -\lambda R/T_{0K} \ln(T/bT_{0K}) \quad (9a)$$

$$\partial(C(T)/T)/\partial(\ln T) = -\lambda R/T_{0K} \quad (9b)$$

which yield the values  $T_{0\rho} \sim 4$  K,  $T_{0\chi} \sim 23$  K, and  $T_{0K} \sim 25$  K. For the fit to  $C(T)/T$  (equation (9a), (9b)), the parameters  $\lambda = 0.251$  and  $b = 0.41$  are taken from the two-channel Kondo model, which has proven to be a useful phenomenological description that yields reasonable values of the scaling temperature  $T_{0K}$  for many NFL systems, although it is not strictly applicable to the present situation from a theoretical point of view. The unusual behavior seen in  $S(T)$  below 5 K also supports the viewpoint that  $T_0$  is in this temperature range. Although the values for  $T_0$  seem to span a wide range of temperatures, this phenomenological scaling

analysis provides a rough estimate of the temperature range through which the system makes a gradual transition into the NFL state.

The low- $T S(T)$  data also imply an unusual state below 5 K. In this measurement,  $T^*$  coincides with the upper limit of the temperature range for NFL behavior. Behnia *et al* [30] have argued that, in the zero-temperature limit, the thermoelectric power should obey the relation,

$$q = \frac{SN_A e}{T\gamma} \quad (10)$$

where  $N_A$  is Avogadro's number,  $e$  is the electron charge and the constant  $N_A e = 9.65 \times 10^4$  C mol<sup>-1</sup> is the Faraday number. The dimensionless quantity  $q$  corresponds to the density of carriers per formula unit for the case of a free-electron gas with an energy-independent relaxation time. In our case,  $q = -2.2$  and differs by sign from all eight cerium compounds considered in [30]. This unusual result may also be indicative of an NFL state at low temperatures.

A comparison to typical heavy-fermion systems may be made by computing an effective Wilson–Sommerfeld ratio,  $R_W = (\pi^2 k_B^2 / 3 \mu_{eff}^2) (\chi_0 / \gamma)$ . Since unambiguous choices for  $\chi_0$  and  $\gamma$  are not obvious, the values  $\chi(H = 10$  kOe),  $\chi_{lin}$ , and  $\gamma$  are taken at 1.9 K to probe the low-temperature state. Also, the Hund's rule effective magnetic moment  $\mu_{eff} = 2.54 \mu_B$  for  $Ce^{3+}$  ions is used. From these values,  $R_W$  is calculated to be  $\sim 0.46$  and  $\sim 0.06$  for  $\chi(H = 10$  kOe) and  $\chi_{lin}$ , respectively. The first value is similar to those found in f-electron materials that exhibit Fermi liquid behavior with heavy quasi-particles, while the second value seems far too low to be physically meaningful. This result suggests that the behavior of  $\chi(T)$  in low fields is intrinsic and the curvature in the isothermal  $M(H)$  curves at low temperatures is not due to paramagnetic impurities.

In typical discussions of NFL physics in f-electron materials, the phenomena are described in terms of interactions between the itinerant electrons and the magnetic rare-earth ions. Examples include: (1) nearness to various types of magnetic quantum critical points where a second-order phase transition is suppressed to 0 K and quantum fluctuations govern physical properties [31, 32]; (2) Kondo disorder, where a range of Kondo temperatures are allowed including  $T_K = 0$  K [33–35]; (3) the Griffiths phase model [36]; and (4) the quadrupolar Kondo model [37]. These pictures have been moderately successful in describing numerous NFL systems [16]. If the viewpoint is taken that the Ce ions are in the magnetic 3+ valence state, then one of these models may be appropriate for describing the low- $T$  behavior. In such a picture, it must be assumed that the anomalous  $\chi(T)$  behavior is due to some unusual phenomena, such as a high  $T_K$ .

However, if the intermediate valence picture is adopted, then Kondo scenarios are unlikely to describe the NFL behavior, since they require the presence of  $Ce^{3+}$  ions. As such, the possibility of a QCP where valence fluctuations on the Ce ions give rise to the incipient NFL state is considered. The existence of a QCP due to a quantum phase transition from integral to intermediate valence has been conjectured in a few other compounds, most notably  $CeCu_2Si_2$ ,  $CeCu_2Ge_2$ ,

CePd<sub>2</sub>Si<sub>2</sub>, and the alloy CeCu<sub>2</sub>(Si<sub>1-x</sub>Ge<sub>x</sub>)<sub>2</sub> [38–43]. The low-pressure region of the  $T$ – $P$  phase diagram for these compounds is similar to that seen for heavy-fermion superconductors such as CeIn<sub>3</sub> and CeMIn<sub>5</sub> ( $M = \text{Co, Rh}$ ), where antiferromagnetic order is suppressed with increasing pressure towards a QCP, around which a superconducting dome is observed at low temperatures [44–46]. Higher pressures then tune the Ce ion from integral to intermediate valence, resulting in a second superconducting dome near a QCP associated with the valence transition. The region surrounding the superconducting dome maximum is also accompanied by NFL behavior. By comparison, an analogous description may be applicable for CeRu<sub>4</sub>As<sub>12</sub> where pressure, magnetic field, or chemical substitution tune the dynamic intermediate valence state.

Finally, it is noteworthy that a recent study shows that  $\rho(T)$  for polycrystalline specimens of CeRu<sub>4</sub>As<sub>12</sub> exhibit thermally activated behavior  $\rho \sim \exp(\Delta/T)$  where  $\Delta = 50$  K, while  $\chi(T)$  and  $C(T)/T$  are similar to those reported here [13]. The transition from a weakly insulating state for polycrystalline samples to semi-metallic NFL behavior for single-crystal samples signals that the electronic state of CeRu<sub>4</sub>As<sub>12</sub> is highly sensitive to perturbations, such as Ce filling or structural disorder, that are affected by the sample growth technique or the degree of crystallinity. We also make a comparison to CeOs<sub>4</sub>As<sub>12</sub>, for which  $\rho(T)$  shows semiconducting behavior [47]. A similar situation is seen for CeRhSb<sub>1-x</sub>Sn<sub>x</sub>, where CeRhSb is a Kondo semiconductor and CeRhSn exhibits NFL behavior [48]. In this system, it is possible to tune through a Kondo insulator–NFL quantum critical point as a function of dopant  $x$ . An analogous study would be of interest for the doping series Ce(Ru<sub>1-x</sub>Os<sub>x</sub>)<sub>4</sub>As<sub>12</sub>.

## 5. Summary

Measurements of  $\rho(T)$ ,  $M(H, T)C(T)/T$ , and  $S(T)$  for single crystals of CeRu<sub>4</sub>As<sub>12</sub> reveal anomalous behavior, most notably a nonmagnetic or weakly magnetic behavior, which evolve into NFL phenomena at low temperatures. As such, CeRu<sub>4</sub>As<sub>12</sub> may be a member of the class of materials whose close proximity to a QCP precipitates NFL behavior. However, the lack of any readily identifiable magnetic quantum critical point suggests that the quantum critical behavior is due to another type of transition, such as a valence transition or metal–insulator transition suppressed to 0 K. Measurements of the electrical resistivity, thermoelectric power, specific heat, and magnetization as a function of pressure, magnetic field, and chemical substitution may yield insight into the nature of the quantum critical behavior in this compound.

## Acknowledgments

This work was supported by the US Department of Energy under grant no. DE FG02-04ER46105 and the National Science Foundation under grant no. NSF DMR0335173 as well as the Polish Committee for Scientific Research (grant no. 1 P03B 073 27).

## References

- [1] Maple M B, Bauer E D, Frederick N A, Ho P-C, Yuhasz W M and Zapf V S 2003 *Physica B* **328** 29
- [2] Aoki Y, Sugawara H, Harima H and Sato H 2005 *J. Phys. Soc. Japan* **74** 209
- [3] Sugawara H, Osaki S, Kobayashi M, Namiki T, Saha S R, Aoki Y and Sato H 2005 *Phys. Rev. B* **71** 125127
- [4] Braun D J and Jeitschko W 1980 *J. Solid State Chem.* **32** 357
- [5] Braun D J and Jeitschko W 1980 *J. Less-Common Met.* **72** 147
- [6] Takeda M and Ishikawa M 2000 *J. Phys. Soc. Japan* **69** 868
- [7] Bauer E D, Slezarski A, Dickey R P, Freeman E J, Sirvent C, Zapf V, Dilley N R and Maple M B 2001 *J. Phys.: Condens. Matter* **13** 5183
- [8] Dordevic S V, Beach K S D, Takeda N, Wang Y J, Maple M B and Basov D N 2006 *Phys. Rev. Lett.* **96** 017403
- [9] Henkie Z, Maple M B, Pietraszko A, Wawryk R, Cichorek T, Baumbach R E, Yuhasz W M, Ho P-C and Henkie Z 2008 *Int. Conf. on New Quantum Phenomena in Skutterudite and Related Systems*
- [10] Sheldrick G M 1985 *Program for the Solution of Crystal Structures* (Germany: University of Göttingen)
- [11] Sheldrick G M 1987 *Program for Crystal Structure Refinement* (Germany: University of Göttingen)
- [12] Wawryk R and Henkie Z 2001 *Phil. Mag. B* **81** 223
- [13] Sekine C, Hoshi N, Takeda K, Yoshida T, Shirota I, Matsuhiro K, Wakeshima M and Hinatsu Y 2007 *J. Magn. Mater.* **310** 260
- [14] Sales B C, Mandrus D, Chakoumakos B C, Keppens V and Thompson J R 1997 *Phys. Rev. B* **56** 15081
- [15] Sales B C, Chakoumakos B C, Mandrus D, Sharp J W, Dilley N R and Maple M B 1999 *Mater. Res. Soc. Symp. Proc.* **545** 13
- [16] Stewart G R 2001 *Rev. Mod. Phys.* **73** 797
- [17] Maple M B, Seaman C L, Gajewski D A, Dalichouch Y, Barbetta V B, deAndrade M C, Mook H A, Lukefahr H G, Bernal O O and MacLaughlin D E 1994 *J. Low Temp. Phys.* **95** 225
- [18] Maple M B, de Andrade M C, Herrmann J, Dalichouch Y, Gajewski D A, Seaman C L, Chau R, Movshovich R, Aronson M C and Osborn R 1995 *J. Low Temp. Phys.* **99** 224
- [19] Lukefahr H G, Bernal O O, MacLaughlin D E, Seaman C L, Maple M B and Andraka B 1995 *Phys. Rev. Lett.* **52** 3038
- [20] Maple M B and Wohlleben D 1971 *Phys. Rev. Lett.* **27** 511
- [21] Maple M B and Wohlleben D 1974 *Magnetism and Magnetic Materials (AIP Conf. Proc. (No. 18))* vol 1073 ed C D Graham Jr and J J Rhyne (New York: AIP) p 447
- [22] Huber J G, Fertig W A and Maple M B 1974 *Solid State Commun.* **15** 453
- [23] Huber J G, Brooks J, Wohlleben D and Maple M B 1974 *Magnetism and Magnetic Materials (AIP Conf. Proc. (No. 24))* (New York: AIP) p 475 (Research article)
- [24] Bridges F *et al* 2008 in preparation
- [25] Seaman C L, Maple M B, Lee B W, Ghamaty S, Torikachvili M S, Kang J-S, Liu L Z, Allen J W and Cox D L 1991 *Phys. Rev. Lett.* **67** 2882
- [26] Dickey R P, Amann A, Freeman E J, de Andrade M C and Maple M B 2000 *Phys. Rev. B* **62** 3979
- [27] Allen J W and Martin R 1982 *Phys. Rev. Lett.* **49** 1106
- [28] Ocko M, Geibel C and Steglich F 2001 *Phys. Rev. B* **64** 195107
- [29] Zlatić V and Monnier R 2005 *Phys. Rev. B* **71** 165109
- [30] Behnia K, Jaccard D and Flouquet J 2004 *J. Phys.: Condens. Matter* **16** 5187
- [31] Hertz J A 1973 *Phys. Rev. B* **14** 1165
- [32] Millis A J 1993 *Phys. Rev. B* **48** 7183

- [33] Bernal O O, MacLaughlin D E, Lukefahr H G and Andraka B 1995 *Phys. Rev. Lett.* **75** 2023
- [34] Miranda E, Dobrosavljevic V and Kotliar G 1996 *J. Phys.: Condens. Matter* **8** 9871
- [35] Miranda E, Dobrosavljevic V and Kotliar G 1997 *Phys. Rev. Lett.* **78** 290
- [36] Castro Neto A H, Castilla G and Jones B A 1998 *Phys. Rev. Lett.* **81** 3531
- [37] Cox D L 1987 *Phys. Rev. Lett.* **59** 1240
- [38] Yuan H Q, Grosche F M, Deppe M, Geibel C, Sparn G and Steglich F 2003 *Science* **302** 2104
- [39] Holmes A, Jaccard D and Miyake K 2004 *Phys. Rev. B* **69** 024508
- [40] Vargoz E and Jaccard D 1998 *J. Magn. Magn. Mater.* **177–181** 294–5
- [41] Raymond S and Jaccard D 2000 *Phys. Rev. B* **61** 8679
- [42] Onodera A, Tsuduki S, Ohishi Y, Watanuki T, Ishida K, Kitaoka Y and Onuki Y 2002 *J. Solid State Commun.* **123** 113–6
- [43] Onishi Y and Miyake K 2001 *J. Phys. Soc. Japan.* **69** 3955
- [44] Walker I R, Grosche F M, Freye D M and Lonzariach G G 1997 *Physica C* **282–287** 303
- [45] Hegger H, Petrovic C, Moshopoulou E G, Hundley M F, Sarrao J L, Fisk Z and Thompson J D 2000 *Phys. Rev. Lett.* **84** 4986
- [46] Jeffries J R, Frederick N A, Bauer E D, Kimura H, Zapf V S, Hof K-D and Sayles T A 2005 *Phys. Rev. B* **72** 024551
- [47] Maple M B, Henkie Z, Baumbach R E, Sayles T A, Butch N P, Ho P-C, Yanagisawa T, Yuhasz W M, Wawryk R, Cichorek T and Pietraszko A 2007 *J. Phys. Soc. Japan* at press
- [48] Slebarski A and Spalek J 2005 *Phys. Rev. Lett.* **95** 046402